Available online at www.sciencedirect.com
ScienceDirect
Applied Catalysis B: Environmental 82 (2008) 219–224
APPLIED CATALYSIS B: ENVIRONMENTAL
www.elsevier.com/locate/apcatb

Nb_2O_5 as efficient and recyclable photocatalyst for indigo carmine degradation

Alexandre G.S. Prado *, Lucas B. Bolzon, Carolina P. Pedroso, Aline O. Moura, Leonardo L. Costa

Instituto de Química, Universidade de Brasília, Caixa Postal 4478, 70904-970 Brasília, DF, Brazil

Received 2 October 2007; received in revised form 14 December 2007; accepted 25 January 2008
Available online 5 February 2008

Abstract

Heterogeneous photocatalysis is a significant green technology for application in water purification. The application of Nb_2O_5 catalyst for the photodegradation of contaminants is few reported in the literature. Thus, the Nb_2O_5 catalyst was characterized by SEM, FTIR, surface area and charge surface density. This catalyst was applied to degrade indigo carmine dye, which was compared with degradation catalyzed by TiO_2 and ZnO. Almost 100% of dye degradation occurred at 20, 45 and 90 min for TiO_2, ZnO and Nb_2O_5, respectively. The effect of Nb_2O_5 catalyst concentration, pH and ionic strength (μ) was investigated. The Nb_2O_5 activity increased at 0.7 g/L and for higher catalyst concentrations the degradation was kept constant. Degradation of indigo carmine dye catalyzed by Nb_2O_5 was improved at pH < 4.0 and μ = 0.05 mol/L. TiO_2, ZnO and Nb_2O_5 were recovered and re-applied in other nine reaction cycles. While TiO_2 and ZnO have an abrupt loss of their catalytic activity, Nb_2O_5 maintained 85% of catalytic activity after 10 reaction cycles.

Keywords: Nb_2O_5; Photodegradation; Dye

1. Introduction

The photoinduced water cleavage on TiO_2 electrodes was discovered by Fujishima and Honda [1]. Since the publication of this paper, a myriad of studies have been developed using TiO_2 and other semiconductors for degradation of organic compounds in water and in air [2–5]. Thus, the heterogeneous photocatalytic oxidation using semiconductors as catalysts becomes an elegant alternative for environmental remediation technology, which offers several advantages over conventional technologies such as the organic pollutant degradation into innocuous final products (e.g., CO_2 and H_2O) [6,7]. Among the organic contaminants, dyes must be highlighted, because they can present toxic effects. Besides, they prevent light penetration in contaminated water. One of most industrial dyes is the indigo carmine dye, which is extensively used as textile colouring agent and widely used in the dyeing of clothes. Thus, environmental studies are necessary to remove this contaminant from water [8].

In these reactions, pure or doped metal oxide semiconductors (e.g., TiO_2 and ZnO) are commonly used as photocatalysts [9,10]. An important step of the photoreaction is the formation of electron–hole pairs, which needs energy to overcome the band gap between the valence and conduction bands (Fig. 1) [11]. Electron–hole pairs are created at the semiconductor surface by irradiation, thus, a charge will transfer between electron–hole pairs and adsorbed species (reactants) onto semiconductor surface, resulting in the photodegradation of contaminants. Among the semiconductors, TiO_2 is the most suitable for the photodegradation of contaminants due to its chemical stability, low cost and low band gap value (3.2 eV). On the other hand, TiO_2 forms hydrocolloids with high stability in water, which favors the catalytic activity. However, such stability difficult the separation of this catalyst from water. Recuperation and re-application of catalysts in other decontamination reactions is part of the green chemistry principles and, in this sense, the use of Nb_2O_5 catalyst can be a new alternative for the photodegradation of contaminants. Considering that Nb_2O_5 presents a band gap value similar to that of TiO_2 (Fig. 1), and that Nb_2O_5 hydrocolloid is not stable, it can be concluded that this catalyst is easily recycled. Due to its acid character

* Corresponding author. Tel.: +55 61 3307 2156; fax: +55 61 3273 4149.
E-mail address: agspradus@gmail.com (A.G.S. Prado).

0926-3373/$ – see front matter © 2008 Elsevier B.V. All rights reserved.
doi:10.1016/j.apcatb.2008.01.024

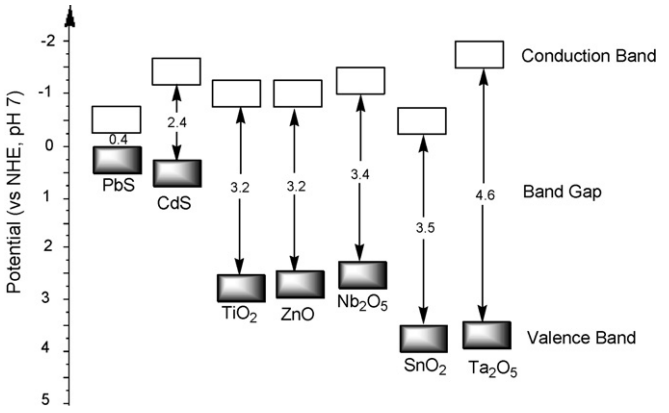

Fig. 1. Position of conduction and valence bands and band gap values for some semiconductors.

[12], Nb_2O_5 is widely used as catalyst in a myriad of reactions such as dehydration [13], hydration [14], etherification [15], hydrolysis [16], condensation [17], alkylation [18], dehydrogenation [19], and mainly, oxidation reactions [20,21]. However, the application of Nb_2O_5 for the photodegradation of contaminants is not well explored in the literature [22–24].

In this direction, this present paper reports the application and re-application of Nb_2O_5 in the photodegradation of indigo carmine dye.

2. Experimental

2.1. Chemicals

Niobium pentoxide (CBMM), carmine indigo (Vetec), TiO_2 (Acros), ZnO (Merck), NaCl (Vetec), NaOH (Vetec) and HNO_3 (Vetec) were used without further purification.

2.2. Characterization of Nb_2O_5 photocatalyst

Scanning electron microscopy (SEM) was performed on a Zeiss EVO 50 microscope. The samples were coated with carbon using a Bal-Tec SCD-050 sputtering system. The equipment was operated at 20 keV.

The surface area was calculated by the Brunauer–Emmett–Teller (BET) method from Nitrogen adsorption–desorption data, which were measured on a Quantachrome Nova 2200 analyzer.

The FTIR spectrum of the solid samples was obtained on a Brucker Equinox 55. The resulting spectrum was the sum of 64 scans. The spectral resolution was 4 cm^{-1}.

The surface charge density of Nb_2O_5 catalyst as a function of pH was calculated by applying Eq. (1) and using the K_1 and K_2 values obtained from simultaneous potentiometric and conductimetric titrations [25,26]. These titrations were carried out with 50.0 mL of a 40.0 g/L Nb_2O_5 aqueous suspension. Firstly, the Nb_2O_5 was fully deprotonated by addition of 0.4 mL of a 1.0 mol/L NaOH solution. This sample was titrated with a 0.1 mol/L solution of HNO_3. The potentiometric readings were done with a PHS-3B pHmeter pHtek and the conductivity was measured with a Cole Parmer conductometer.

2.3. Indigo carmine photocatalytic degradation

Photolysis of indigo carmine dye was carried out in a homemade photo-reactor (Fig. 2) [27] using 100.0 mL of a 2.5×10^{-5} mol/L dye solution and 1.0 g/L of the Nb_2O_5, TiO_2 and ZnO catalysts. These solutions were illuminated with a 125 W mercury-vapour lamp OSRAM HQL 125 with temperature being monitored during the reaction. The irradiation intensity per time was monitored by Instrutherm UV-MRU-201 radiometer, which was 15 J cm^{-2} during 3 h of experiment. The dye degradation was followed on a Beckman DU-650 UV–vis spectrophotometer.

2.4. Effect of Nb_2O_5 photocatalyst concentration

About 100.0 mL of a 2.5×10^{-5} mol/L dye solution containing different concentrations of Nb_2O_5 (from 0 to 4.0 g/L) was illuminated in a photo-reactor for 60 min.

2.5. Effect of ionic strength

About 100.0 mL of a 2.5×10^{-5} mol/L dye and 0.1 g/L Nb_2O_5 solution was used to degrade a 1.0×10^{-5} mol/L indigo carmine dye solution at different ionic strength values, which were adjusted by addition of NaCl. Irradiation in a photo-reactor was carried out for 60 min.

2.6. Effect of pH

About 100.0 mL of a 2.5×10^{-5} mol/L dye and Nb_2O_5 0.1 g/L solution was used to degrade a 1.0×10^{-5} mol/L indigo carmine dye solution at different pH values, which were adjusted by addition of HCl or NaOH. Irradiation in a photo-reactor was carried out for 60 min.

2.7. Recycling of Nb_2O_5 compared with ZnO and TiO_2

After each indigo carmine photodegradation reaction, solution was centrifuged by Centrebio Model 80-2B with a rotation of 4000 rpm for 2 h. Solid phase was carefully separated, and the liquid phase was filtered off by a simple filtration system by using filter paper Quanty JP-41 black belt with density of 80 g cm^{-3}, 28 μm of porous diameter, and air permeability of 55 L s^{-1} m^{-2}. Then, the separated catalyst was added again to a photo-reactor to be used in the subsequent reactions.

3. Results

3.1. Characterization

The SEM images were acquired in order to understand the morphology of the Nb_2O_5 particles. A representative SEM image of this catalyst is depicted in Fig. 3 which shows that the Nb_2O_5 particles are very polydisperse, so, the particles sizes could not be correctly determined. However, the most of the particles presented sizes ranging from 2 to 20 μm.

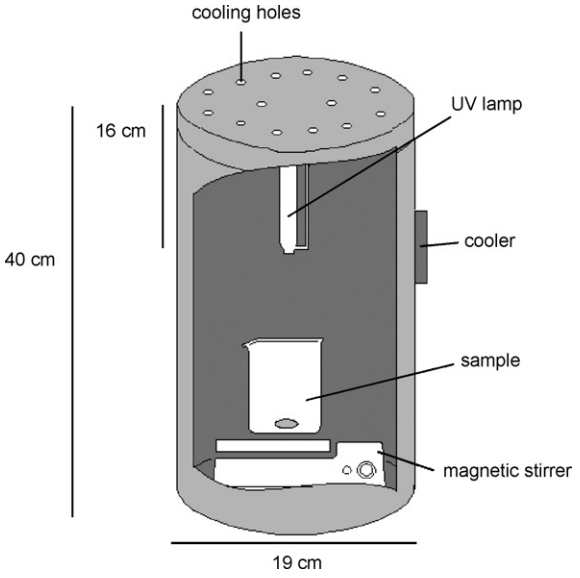

Fig. 2. Schematic draw of home-made photo-reactor.

The FTIR spectrum of Nb_2O_5 (Fig. 4) presents the characteristic peaks of this catalyst: a peak at 3530 cm^{-1} assigned to the OH stretching of Nb–OH, a broad band between 1700 and 1500 cm^{-1} related to adsorbed water on the Nb_2O_5 surface, a shoulder at 953 cm^{-1} and a peak 880 cm^{-1} assigned to Nb=O stretchings, and bands between at 700 and 600 cm^{-1} related to Nb–O–Nb angular vibration [28–30].

Fig. 5 shows the nitrogen isotherm of Nb_2O_5, which was classified as a typical Type IV isotherm. A small hysteresis loop in the P/P_0 range of 0.4–1.0 is observed, showing that the adsorption–desorption process is not reversible. This is a consequence of the hysteresis loops caused by the capillary condensation and the pore size. Thus, this isotherm is characteristic of the predominant presence of micropores having mesoporous sites with an agglomerate structure [31–33].

In order to know the effect of pH on Nb_2O_5 surface and, consequently, its catalytic ability, the density charge surface was followed as a function of pH (Fig. 6). The pK_1 and pK_2 values were obtained from potentiometric titration of acidified Nb_2O_5 and applied in Eq. (1) to find the density charge surface

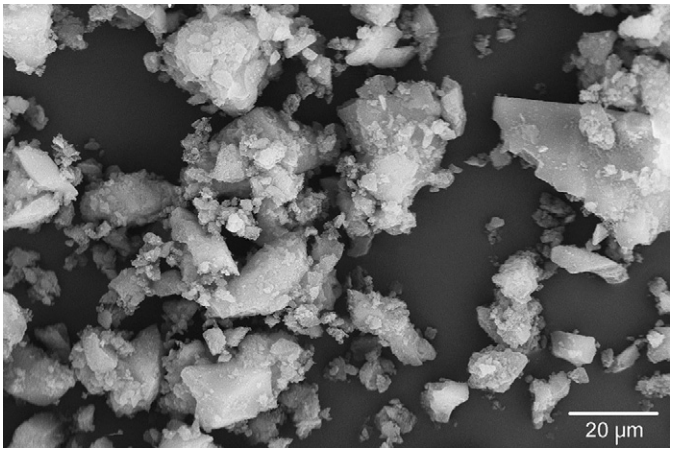

Fig. 3. SEM image of Nb_2O_5 photocatalyst.

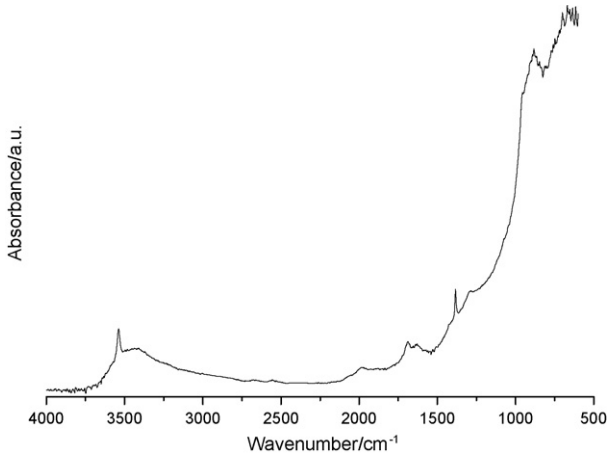

Fig. 4. FTIR spectrum of Nb_2O_5 catalyst.

(ρ_0) [34]:

$$\rho_0 = \frac{F}{A}\left(\frac{10^{-2\mathrm{pH}} - K_1K_2}{10^{-2\mathrm{pH}} + K_1 \times 10^{-\mathrm{pH}} + K_1K_2}\right)N_T \quad (1)$$

where F is the Faraday constant, A is the total surface area, N_T is the total number of moles of surface sites, and K_1 and K_2 correspond to the acid equilibria constants.

Fig. 6 shows three distinct regions. The first region is assigned to the protonated surface corresponding to the MOH_2^+ acid sites up to pH 3.8. The pH values between 3.8 and 5.4 are related to uncharged amphoteric surface sites (MOH). Above pH 5.4, the surface of Nb_2O_5 is fully deprotonated (MO^-). The point of zero charge (pzc) was observed at pH 4.54.

3.2. Photocatalytic activity of Nb_2O_5

The main catalysts used to photodegrade contaminants are TiO_2 and ZnO, both having a band gap of 3.2 eV. Nb_2O_5 has a band gap similar to that of TiO_2 and ZnO catalysts, i.e., 3.4 eV, and has commonly been used as dopant of photocatalysts [35–37]. However, there are few reports in the literature on the application of this oxide in photodegradation [22–24]. Thus, a

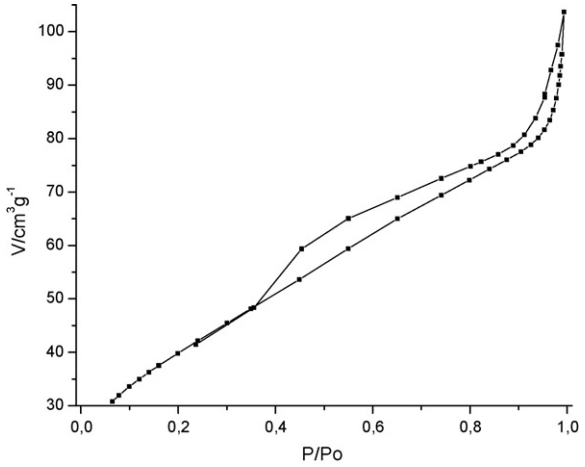

Fig. 5. N_2 Adsorption isotherm of Nb_2O_5.

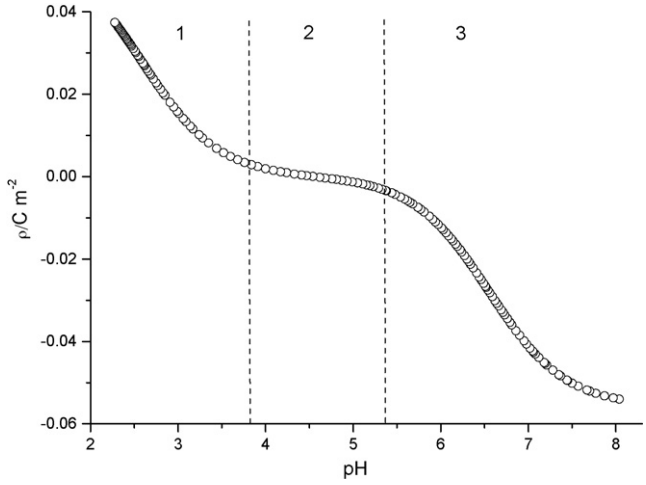

Fig. 6. Variation of density surface charge as a function of pH for Nb_2O_5.

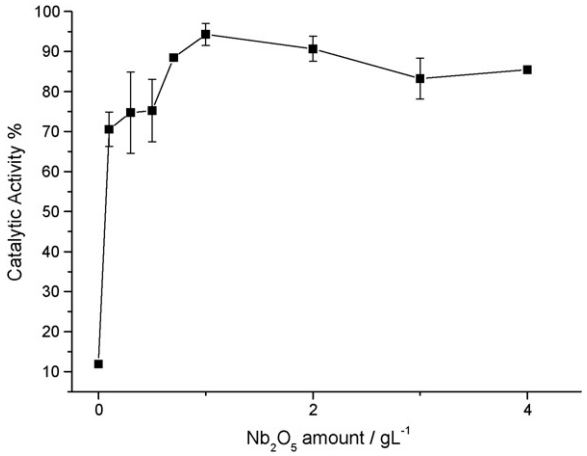

Fig. 8. Photocatalytic activity of Nb_2O_5 as a function of its concentration.

detailed study of the photocatalytic properties of Nb_2O_5 is necessary. In this sense, the degradation of indigo carmine dye was followed as a function of time in the presence of Nb_2O_5 catalyst. Indigo carmine dye degradation was also followed in the presence of TiO_2 and ZnO catalysts in order to evaluate the photocatalytic ability of nobium pentoxide in comparison with the key photocatalysts. Fig. 7 shows that TiO_2 presented high photocatalytic activity to degrade indigo carmine, degrading practically 100% of dye at 25 min of reaction. This ability was followed by ZnO catalyst activity, which degraded almost all dye at 45 min of reaction, while Nb_2O_5 degraded the dye only at 90 min. These results showed that TiO_2 acts faster than ZnO and Nb_2O_5, which could be explained by the high stability of TiO_2 and ZnO hydrocolloids. The low stability of Nb_2O_5 causes the precipitation of the oxide and, as consequence, decreases its catalytic activity. On the other hand, the stability of TiO_2 and ZnO makes their separation from reaction solution difficult. In this sense, the photocatalytic activity of Nb_2O_5 should be more explored, and that is the reason for which some reaction parameters have been studied in this paper.

The effect of Nb_2O_5 concentration on the phtotodegradation of indigo carmine dye was followed, as shown in Fig. 8. It can be seen that the photocatalytic activity increased with Nb_2O_5 concentration up to 0.7 g/L, due to the increase of photon absorption by increase of catalyst amount, which generates more electron–hole pairs, and consequently, increases photodegradation activity [38]. Above this concentration, the activity was kept constant. This fact can be explained by absorption and scattering of light by Nb_2O_5 particles, which decreases light intensity in reaction medium [38].

The effect of ionic strength on the catalytic activity of Nb_2O_5 to degrade indigo carmine dye was followed, as shown in Fig. 9. In the first stage, the addition of salt resulted in a distribution of ions near the Nb_2O_5 surface, leading to a potential difference on the solid/liquid interface [39]. Thus, up to an ionic strength of 0.05 mol/L (NaCl), it was verified a colloidal stabilization of Nb_2O_5. The colloidal stabilization reflects directly on the catalytic activity of Nb_2O_5, due to a large amount of oxide suspended in water capable of catalyzing the indigo carmine degradation. Above this ionic strength value, the double layer thickness must be decreased, and at high salt concentration the double layer collapses to an extent that the ever-present attractive van der Walls forces overcome the charge repulsion [40]. Indeed, electrostatically stabilized colloidal suspensions

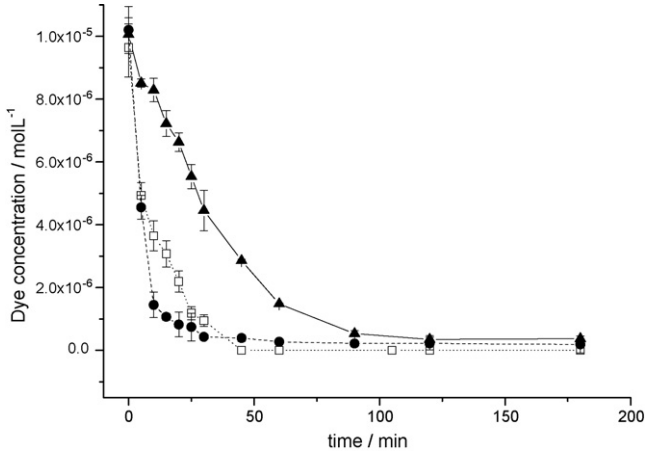

Fig. 7. Kinetics of photocatalytic degradation of 1×10^{-5} mol/L indigo carmine dye solution using 1.0 g/L of ZnO (□), TiO_2 (●) and Nb_2O_5 (▲).

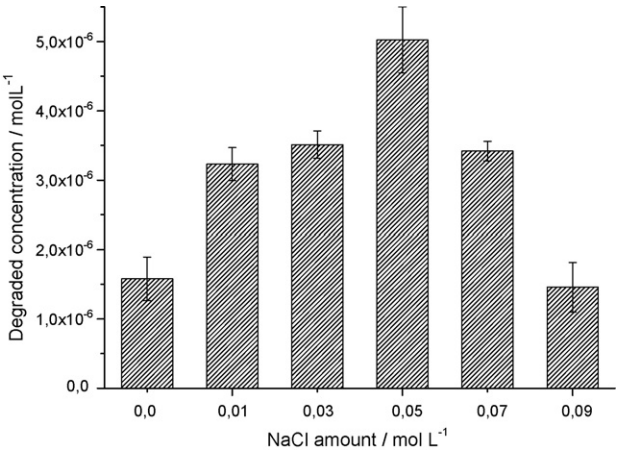

Fig. 9. Photodegradation of indigo carmine dye by Nb_2O_5 as a in function of NaCl amount in solution.

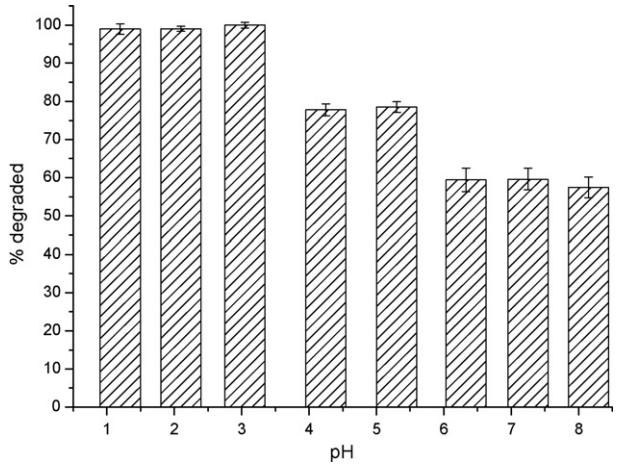

Fig. 10. Photodegradation of indigo carmine by Nb_2O_5 with different mean pH values.

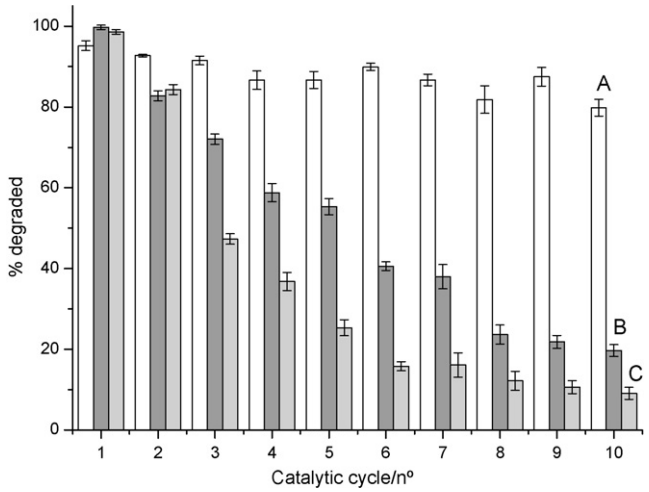

Fig. 12. Catalytic yields of Nb_2O_5 (A), ZnO (B) and TiO_2 (C) as a function of their re-application.

of Nb_2O_5 became unstable upon addition of 0.05 mol/L of NaCl. The double layer collapse results in the precipitation of niobium pentoxide and, as consequence, the photocatalytic activity of Nb_2O_5 decreased above 0.05 mol/L of NaCl.

The effect of pH values on the photodegradation was also studied, as shown in Fig. 10. The degradation was higher in acid medium (pH 3), with almost all dye being degraded. Up to a value of 5.5, the dye degradation decreased to 80%. Above pH 5.5, the degradation continued to decrease. This catalyst behaviour can be explained by the surface charge density of Nb_2O_5. The Nb_2O_5 surface is fully protonated below pH 4 and is deprotonated for pH values higher than 5.5. Considering the indigo carmine structure (Fig. 11), the positive charge excess in the Nb_2O_5 surface promotes a strong interaction with SO_3^- groups of the dye (Fig. 11a). In the region of the amphoteric sites the interaction is made only by hydrogen bonds and, consequently, is weaker (Fig. 11b). Finally, the negative charge excess promotes the repulsion of the dye by the niobia surface, diminishing the catalytic activity of this semiconductor (Fig. 11c). The surface charge density of Nb_2O_5 shows that its surface is fully protonated in pH < 3.8 (Fig. 6), which corroborates the pH effect on the photocatalytic activity.

The catalyst was recycled and re-applied to degrade the dye. The recycling studies were followed with TiO_2 and ZnO in order to compare catalytic activity of Nb_2O_5, as shown in Fig. 12. These studies revealed that TiO_2 and ZnO recovery is difficult and the re-use of these catalysts is not effective. The activity of ZnO and TiO_2 catalysts decreased drastically to 20 and 10% of dye degradation, respectively, after 10 reaction cycles. On the other hand, Nb_2O_5 maintained 85% of dye

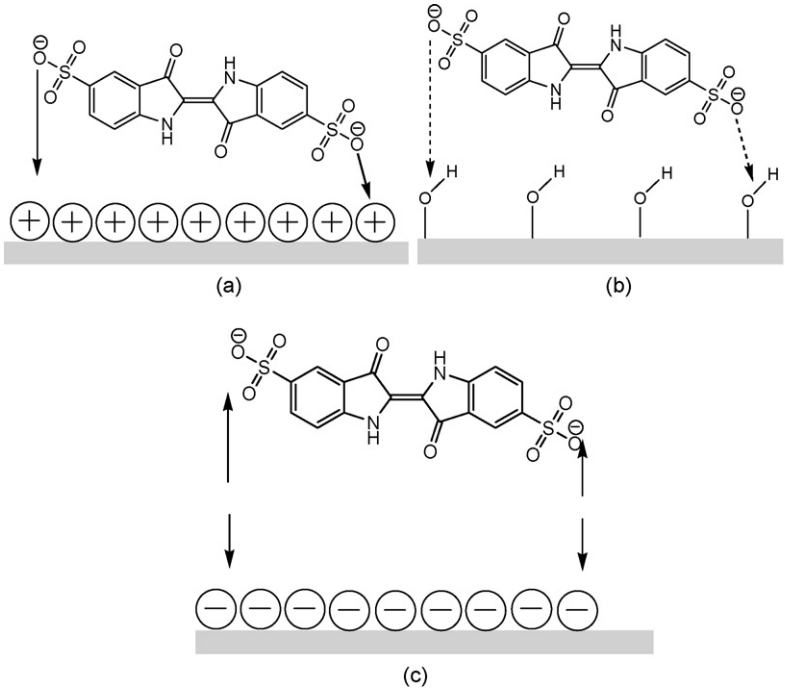

Fig. 11. Schematic interaction model for indigo carmine and Nb_2O_5: (a) acid sites, (b) amphoteric sites and (c) basic sites.

degradation after 10 catalytic cycles, evidencing the Nb_2O_5 ability to be re-applied in photodegradation reactions. This ability goes towards the key principles of green chemistry [41].

4. Conclusion

Nb_2O_5 presented photocatalytic activity to degrade indigo carmine dye. This catalyst presented the best activity at pH < 4 and ionic strength of 0.05 mol L^{-1}. The great advantage of Nb_2O_5 in comparison with other traditional photocatalysts (TiO_2 and ZnO) is its easy recovery and, as consequence, the fact that Nb_2O_5 can be recycled and re-applied in many photodegradation steps, maintaining 85% of activity after 10 cycles of reaction.

Acknowledgments

The authors acknowledge FINATEC, FUNPE/UnB and CT/ENERG for supporting this research. The authors also thank CNPq for the fellowships.

References

[1] A. Fujishima, K. Honda, Nature 238 (1972) 37.
[2] M. Abu Tariq, M. Faisal, M. Muneer, D. Bahnemann, J. Mol. Catal. A 265 (2007) 231.
[3] D.W. Chen, A.K. Ray, Appl. Catal. B 23 (1999) 143.
[4] L. Ge, M.X. Xu, H.B. Fang, J. Mol. Catal. A 258 (2006) 68.
[5] P. Calza, V.A. Sakkas, C. Medana, C. Baiocchi, A. Dimou, E. Pelizzetti, T. Albanis, Appl. Catal. B 67 (2006) 197.
[6] J. Zhao, X. Yang, Build. Environ. 38 (2003) 645.
[7] V.M. Cristante, A.G.S. Prado, S.M.A. Jorge, J.P.S. Valente, A.O. Florentino, P.M. Padilha, J. Photochem. Photobiol. A 195 (2008) 23.
[8] A.G.S. Prado, B.S. Miranda, G.V.M. Jacintho, Surf. Sci. 542 (2003) 276.
[9] M.R. Hoffmann, S.T. Martin, W. Choi, D.W. Bahnemannt, Chem. Rev. 95 (1995) 69.
[10] E. Evgenidou, K. Fytianos, I. Poulios, Appl. Catal. B 59 (2005) 81.
[11] H.H. Kung, H.S. Jarrett, A.W. Sleight, A. Ferretti, J. Appl. Phys. 48 (1977) 2463.
[12] E.A. Faria, A.G.S. Prado, React. Funct. Polym. 67 (2007) 655.
[13] P. Carniti, A. Gervasini, S. Biella, A. Auroux, Catal. Today 118 (2006) 373.
[14] Y. Li, S. Yan, L. Qian, W. Yang, Z. Xie, Q. Chen, B. Yue, H. He, J. Catal. 241 (2006) 173.
[15] T.A. Peters, N.E. Benes, A. Holmen, J.T.F. Keurentjes, Appl. Catal. A 297 (2006) 182.
[16] T. Okuhara, M. Kimura, T. Kawai, Z. Xu, T. Nakato, Catal. Today 45 (1998) 73.
[17] M. Paulis, M. Martin, D.B. Soria, A. Diaz, J.A. Odriozola, M. Montes, Appl. Catal. A 180 (1999) 411.
[18] K. Yamashita, M. Hirano, K. Okumura, M. Niwa, Catal. Today 118 (2006) 385.
[19] J.B. de Paiva, W.R. Monteiro, M.A. Zacharias, J.A.J. Rodrigues, G.G. Cortez, Braz. J. Chem. Eng. 23 (2006) 517.
[20] V.S. Braga, F.A.C. Garcia, J.A. Dias, S.C.L. Dias, J. Catal. 247 (2007) 68.
[21] F.B. Noronha, D.A.G. Aranda, A.P. Ordine, M. Schmal, Catal. Today 57 (2000) 275.
[22] H. Kominami, K. Oki, M. Kohno, S. Onoue, Y. Kera, B. Ohtani, J. Mater. Chem. 11 (2001) 604.
[23] A.G.S. Prado, E.A. Faria, J.R. SouzaDe, J.D. Torres, J. Mol. Catal. A 237 (2005) 115.
[24] J.D. Torres, E.A. Faria, J.R. SouzaDe, A.G.S. Prado, J. Photochem. Photobiol. A 182 (2006) 202.
[25] N. Kallay, T. Madic, K. Kucej, T. Preocanin, Colloids Surf. A 250 (2004) 289.
[26] G.A. Parks, P.L.D. Bruyn, J. Phys. Chem. 66 (1962) 967.
[27] L.B. Bolzon, J.R. SouzaDe, A.G.S. Prado, Rev. Bras. Ens. Quím. 1 (2006) 25.
[28] L.J. Burcham, J. Datka, I.E. Wachs, J. Phys. Chem. B 103 (1999) 6015.
[29] J.M. Jehng, I.E. Wachs, Chem. Mater. 3 (1991) 100.
[30] V.S. Braga, J.A. Dias, S.C.L. Dias, J.L. Macedo, Chem. Mater. 17 (2005) 690.
[31] E. DeOliveira, A.G.S. Prado, J. Mol. Catal. A 271 (2007) 63.
[32] P. Klobes, H. Preiss, K. Meyer, D. Shultze, Mikrochim. Acta 125 (1997) 343.
[33] A.K.H. Norman, H.M. Ismail, Colloids Surf. A 136 (1998) 237.
[34] A.F.C. Campos, F.A. Tourinho, G.J. Silva, M.C.F.L. Lara, J. Depeyrot, Eur. Phys. J. E 6 (2001) 29.
[35] H.Y. Xiao, Q.X. Dai, W.S. Li, C.T. Au, X.P. Zhou, J. Mol. Catal. A 245 (2006) 17.
[36] H. Cui, K. Dwight, S. Soled, A. Wold, J. Solid State Chem. 115 (1995) 187.
[37] G.B. Saupe, Y. Zhao, J. Bang, N.R. Yesu, G.A. Carballo, R. Ordonez, T. Bubphamala, Microchem. J. 81 (2005) 156.
[38] Y. Zang, R. Farnood, Appl. Catal. B 57 (2005) 275.
[39] P.A. Albertsson, Partition of Cell Particles and Macromolecules, third ed., John Wiley & Sons, New York, 1985.
[40] W. Stumm, J.J. Morgan, Aquatic Chemistry: An Introduction Emphasizing Chemical Equilibria in Natural Waters, John Wiley & Sons, New York, 1981.
[41] A.G.S. Prado, Quim. Nova 26 (2003) 738.